

Journal Pre-proof

Tris(β -ketoiminato)ruthenium(III) complexes: Electrochemical and computational chemistry study

Tankiso Lawrence Ngake, Johannes H. Potgieter, Jeanet Conradie



PII: S0013-4686(19)31494-X

DOI: <https://doi.org/10.1016/j.electacta.2019.134635>

Reference: EA 134635

To appear in: *Electrochimica Acta*

Received Date: 27 April 2019

Revised Date: 29 July 2019

Accepted Date: 1 August 2019

Please cite this article as: T.L. Ngake, J.H. Potgieter, J. Conradie, Tris(β -ketoiminato)ruthenium(III) complexes: Electrochemical and computational chemistry study, *Electrochimica Acta* (2019), doi: <https://doi.org/10.1016/j.electacta.2019.134635>.

This is a PDF file of an article that has undergone enhancements after acceptance, such as the addition of a cover page and metadata, and formatting for readability, but it is not yet the definitive version of record. This version will undergo additional copyediting, typesetting and review before it is published in its final form, but we are providing this version to give early visibility of the article. Please note that, during the production process, errors may be discovered which could affect the content, and all legal disclaimers that apply to the journal pertain.

© 2019 Published by Elsevier Ltd.

Tris(β -ketoiminato)ruthenium(III) complexes: Electrochemical and computational chemistry study

Tankiso Lawrence Ngake,¹ Johannes. H. Potgieter^{2,3*} and Jeanet Conradie^{1*}

1. Department of Chemistry, University of the Free State, P.O. Box 339, Bloemfontein, 9300, South Africa

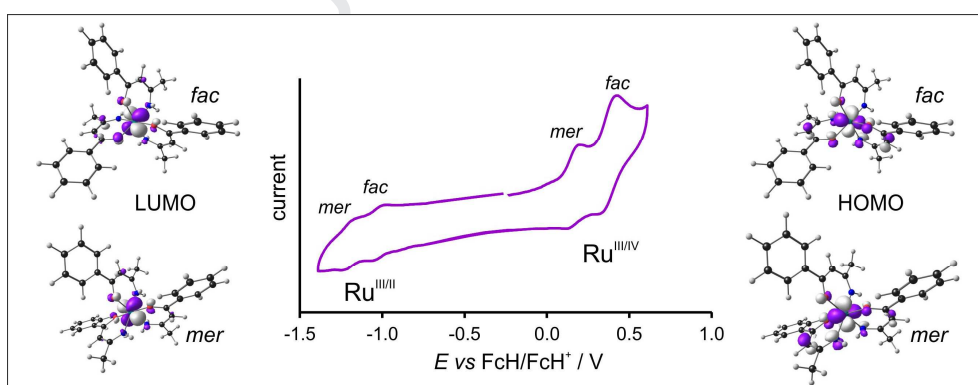
2. Division of Chemistry and Environmental Science, Manchester Metropolitan University, Manchester, M1 5GD, UK

3. School of Chemical and Metallurgical Engineering, University of the Witwatersrand, Private Bag X3, Wits, 2050, South Africa

Contact author details:

Name: Jeanet Conradie, Tel: ++27-51-4012194, Fax: ++27-4017295, email: conradj@ufs.ac.za

SYNOPSIS TOC



SYNOPSIS TEXT

Electrochemical and computational chemistry study of the *fac* and *mer* isomers of tris(β -ketoiminato)ruthenium(III) complexes:

- Ru^{III/IV}, Ru^{III/II} redox couples, as well as ligand based reduction of Ru^{II} complex
- Separate Ru^{III/IV} redox couples for *fac* and *mer* isomers
- DFT calculations provide understanding of the locus of the observed redox couples

Abstract

The electronic and electrochemical properties are reported here for the first time for a series of five tris(β -ketoiminato)ruthenium(III) complexes. Since the β -ketoiminato ligand is unsymmetrical, both *fac* and *mer* isomers are theoretically possible for these octahedral complexes. Density functional theory calculations show that for complexes containing an H on the imino position, both the *fac* and *mer* are energetically possible, while for complexes with a Ph on the imino position, the *mer* isomer is energetically favoured, due to the steric hindrance caused by the Ph group in the *fac* isomer. Electrochemistry, utilizing cyclic voltammetry, showed Ru^{III/IV} oxidation, Ru^{III/II} reduction, as well as ligand based reduction of the Ru^{II} complex. Different Ru^{III/IV} and Ru^{III/II} redox couples were observed for the different *fac* and *mer* isomers of the tris(β -ketoiminato)ruthenium(III) complexes.

Keywords

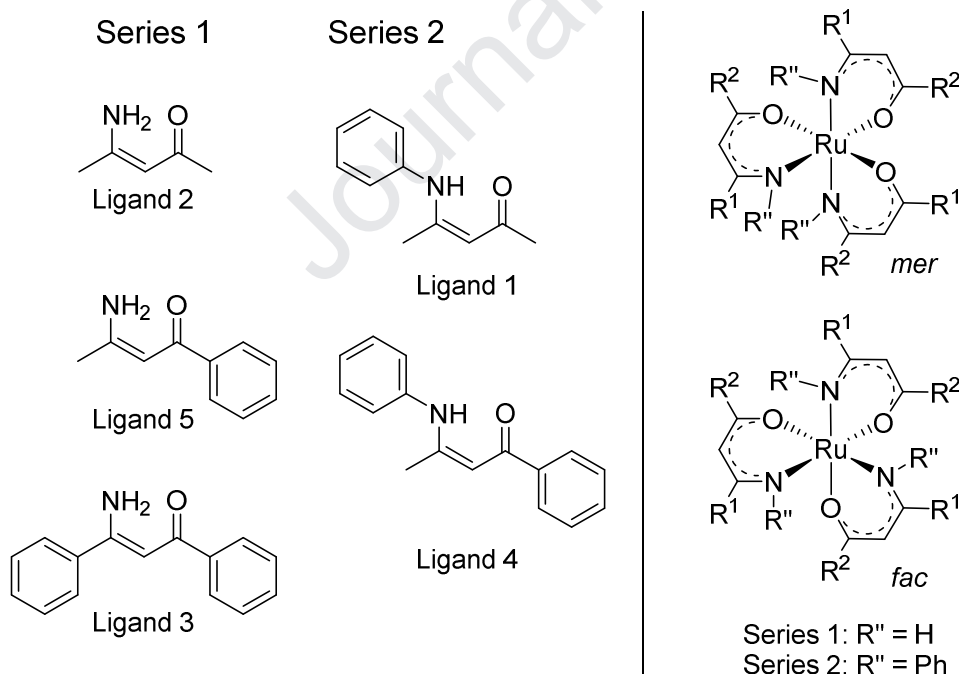
bidentate N,O ligands; β -ketoimine; ruthenium(III); Redox potential; DFT

1 Introduction

Ruthenium complexes containing N,N, N,O or O,O bidentate ligands have been extensively studied before, for example in their use as potential anti-cancer agents [1]. The N,O bidentate ligand-containing Ru-complexes have been studied for their photophysical properties [2] and for their use in the catalytic dehydrogenation of benzoyl amine as co-oxidant [3]. The N,N bidentate ligand-containing Ru-complexes have been studied for artificial photosynthesis purposes and excited state properties [4]. Furthermore, Ru-complexes containing these N,N bidentate ligands such as (2,2'-bipyridine, 1-10-phenanthroline) are used as dye-sensitizers for solar cells [5]. On the other hand, metal complexes containing O,O bidentate ligands (such as acetyl acetone) are used in catalysis [6] and as electrolyte in non-aqueous redox flow batteries [7]. All these complexes have attracted a lot of interest because of their favourable photophysical and electrochemical properties, which can be systematically fine-tuned to achieve optimal customized material characteristics. In

the event where these complexes are studied for their catalytic properties, it is of importance especially for industries, to study the factors that influence the activity of a catalyst towards oxidation, reduction, substitution or oxidative addition, in order to develop more effective, cheaper and more earth-abundant catalysts [8]. As yet not much attention has been given to the electrochemical properties of the ruthenium complexes containing N,O bidentate ligands (N,O-BID), therefore it is of great importance to also study electrochemical properties of such complexes. It has been previously shown that complexes with nitrogen as donor atom preferably coordinate with metals above those complexes with oxygen as donor atom [9]. It therefore will be interesting to study the electronic influence of both the ligand substituents as well as the two donor atoms N and O of the bidentate ligands, N,O-BID, on the metal they are coordinated to (metal-N,O-BID complex), comparing them with the related metal-O,O-BID complexes.

In this study we thus present an electrochemical and computational chemistry study of five novel tris(β -ketoiminato)ruthenium(III) complexes, containing amino substituted β -amino α,β -unsaturated ketones (bidentate N,O-ligands), see **Scheme 1**. The electronic influence of the phenyl group (on the metal complex) in different positions on the ligand are highlighted. These complexes have two geometrical isomers, meridian (*mer*) and facial (*fac*), see **Scheme 1**.



Scheme 1. Structure of the β -ketoimine ligands L1 – L5, as well as the *fac* and *mer* isomers of the corresponding tris(β -ketoiminato)ruthenium(III) complexes 1 – 5 of this study (with the two groups R^1 and R^2 on the ligand being either CH_3 or Ph). Series 1 exists of complexes 2, 3 and 5, containing ligands L2, L3 or L5 with group $R'' = \text{H}$, while Series 2 exists of complexes 1 and 4, containing ligands L1 or L4 with group $R'' = \text{Ph}$ (where the group on the N atom is R'').

2 Experimental

2.1 General

UV/vis spectra were recorded on a Varian Cary 50 Conc ultra-violet/visible spectrophotometer. MS was recorded on an ABSCIEX 4000QTRAP or Bruker Microflex LRF20 spectrophotometer. Proton NMR were recorded on a 300 MHz Bruker FOURIER NMR spectrometer operating at 25°C, ^1H frequency = 300.18 MHz. Chemical shifts are reported relative to tetramethylsilane $\text{Si}(\text{CH}_3)_4$ at 0.00 ppm. Solid state Fourier transform infrared measurements were performed on a Thermo Scientific Nicolet iS50 Attenuated Total Reflectance Fourier transform infrared (ATR-FTIR) spectrometer using the iS50 ATR option running OMNIC software (Version 9.2).

2.2 Synthesis

The five bidentate N,O-ligands were synthesized and characterized as reported for ligands 1, 2, 4 and 5 [10,11]. The synthesis of ligand 3 is described below. The five ruthenium complexes of the corresponding ligands were synthesized by using literature methods of related complexes as a guide [22,12].

2.2.1 Ligand 3 (L3)

1,3-diphenylpropane-1,3-dione (2.438 g, 10.9 mmol) was dispersed over Montmorillonite K-10 (2 g) and DCM (20 ml) was added. While stirring, a mixture of ammonia solution (0.35 ml, 20.5 mmol) and DCM (10 ml) was added. The reaction was stirred at room temperature for 24 hours. The catalyst was removed by filtration and the solvent was firstly removed on a rotatory evaporator, then under vacuum, yielding a red powder (1.687 g). Yield 69%. ^1H NMR (300 MHz, CDCl_3 , 25°C): δ 8.03 – 7.49 ppm (m, Ph, 10H); 6.89 ppm (s, C-H, 1H); 5.32 ppm (s, NH, 1H).

2.2.2 $[\text{Ru}(\text{L1})_3]$ (1)

A mixture of L1 (1.951 g, 11.1 mmol) in THF (25 ml) was added dropwise, while stirring, to a mixture of sodium hydride (0.38 g, 15.8 mmol) and THF (25 ml). The reaction mixture was stirred at room temperature for about 30 minutes. The unreacted sodium hydride was removed by

filtration. The filtrate was added to a mixture of $[\text{Ru}(\text{COD})\text{Cl}_2]_2$, (0.82 g, 2.93 mmol) in THF (25 ml) and the mixture was refluxed for 48 hours. The solution was washed with water to eliminate any formed NaCl. The solvent was removed by rotatory evaporator and the resultant crystals were placed under vacuum to yield dark green crystals (0.507 g). Yield 62%. MS Calcd. ($[\text{M}]^+$ positive mode): m/z 624.75. MS Found: m/z 625.3. UV: λ_{max} 325 nm, ϵ_{max} 54847 $\text{mol}^{-1}\text{dm}^3\text{cm}^{-1}$. Elemental analysis calculated for $\text{RuC}_{33}\text{N}_3\text{H}_{36}\text{O}_3$ (element, %): C, 63.55; H, 5.82; N, 6.74; obtained: C, 63.22; H, 5.49; N, 6.74.

2.2.3 $[\text{Ru}(\text{L2})_3]$ (2)

$\text{RuCl}_3 \cdot 3\text{H}_2\text{O}$ (100 mg, 0.4 mmol) was dissolved in 10 ml of ethanol. The mixture was refluxed for 15-20 minutes until the black colour turned green. A mixture of L2 (0.2970 g, 3 mmol) in 20 ml ethanol was added and the whole reaction mixture was refluxed for 3 hours. The solvent was removed by rotatory evaporator to obtain a dark blue solid (0.1907 g) Yield 64.2%. MS Calcd. m/z 395.44. Found: m/z 395.36. UV: λ_{max} 567, 354 and 279 nm, ϵ_{max} 2164, 8063 and 12597 $\text{mol}^{-1}\text{dm}^3\text{cm}^{-1}$. Elemental analysis calculated for $\text{RuC}_{13}\text{N}_3\text{H}_{24}\text{O}_3$ (element, %): C, 45.56; H, 6.12; N, 10.63; obtained: C, 45.66; H, 5.75; N, 11.61.

2.2.4 $[\text{Ru}(\text{L4})_3]$ (4)

A mixture of $\text{RuCl}_3 \cdot 3\text{H}_2\text{O}$ (100 mg, 0.48 mmol), L4 (0.4556 g, 1.92 mmol) and KOH (215 mg, 3.84 mmol) in methanol (30 ml) was stirred for 24 hours at room temperature. The solvent was removed on the rotatory evaporator. To the dark green solid was added ~10 ml of DCM and the solution was filtered and the solvent was removed from the filtrate. The product was purified by column chromatography on silica (column). The product was eluted by 8:2 DCM:Hexane. Yield: 0.1604 g (35%), MS Calcd. ($[\text{M}]^+$ positive mode): m/z 810.95. Found: m/z 810.2. UV: λ_{max} 355 nm, ϵ_{max} 21189 $\text{mol}^{-1}\text{dm}^3\text{cm}^{-1}$. Elemental analysis calculated for $\text{RuC}_{48}\text{N}_3\text{H}_{42}\text{O}_3$ (element, %): C, 71.18; H, 5.23; N, 5.19; obtained: C, 70.47; H, 6.18; N, 4.72.

2.2.5 $[\text{Ru}(\text{L5})_3]$ (5)

A mixture of $\text{RuCl}_3 \cdot 3\text{H}_2\text{O}$ (100 mg, 0.48 mmol), L5 (0.314 g, 1.95 mmol) and KOH (215 mg, 3.84 mmol) in methanol (30 ml) was stirred for 24 hours at room temperature. The solvent was removed on the rotatory evaporator. To the dark green solid was added ~10 ml of DCM and the solution was filtered and the solvent was removed from the filtrate to yield dark blue solid. Yield: 0.1934 g (62%), MS Calcd. ($[\text{M}]^+$ positive mode): m/z 582.66. Found: m/z 582.5. UV: λ_{max} 305 and

245 nm, ϵ_{\max} 15629 and 21009 mol⁻¹dm³cm⁻¹. Pr

Elemental analysis calculated for RuC₃₀N₃H₃₀O₃ (element, %): C, 61.95; H, 5.20; N, 7.22; obtained: C, 62.26; H, 5.64; N, 7.74.

2.2.6 [Ru(L3)₃](3)

A mixture of L3 (0.784 g, 3.5 mmol) in THF (25 ml) was added dropwise, while stirring, to a mixture of sodium hydride (0.134 g, 5.58 mmol) and THF (25 ml). The reaction mixture was stirred at room temperature for about 30 minutes. The unreacted sodium hydride was removed by filtration. The filtrate was added to a mixture of [Ru(COD)Cl₂]_x (0.275 g, 0.98 mmol) in THF (25 ml) and the mixture was refluxed for 48 hours. The solution was washed with water to eliminate any NaCl formed. The solvent was removed by rotatory evaporator and the resultant powder was placed under vacuum to yield a dark brown powder (0.45 g) Yield 58%. MS Calcd. ([M]⁺ positive mode): *m/z* 768.87. Found: *m/z* 769.2. UV: λ_{\max} 324 and 251 nm, ϵ_{\max} 23688 and 30961 mol⁻¹dm³cm⁻¹. Elemental analysis calculated for RuC₄₅N₃H₃₆O₃ (element, %): C, 70.39; H, 4.73; N, 5.47; obtained: C, 70.07; H, 4.03; N, 5.00.

2.3 Cyclic Voltammetry

Cyclic voltammetric (CV) measurements were conducted on a BAS100B Electrochemical Analyzer linked to a personal computer, utilizing the BAS100W Version 2.3 software. Measurements were done at 293 K and the temperature was kept constant within 0.5 K. Successive experiments under the same experimental conditions showed that all formal reduction and oxidation potentials were reproducible within 0.005 V. Cyclic voltammetric (CV) measurements were performed either on a concentration of 2 mmol dm⁻³ or on saturated solutions of each of the five complexes, dissolved in CH₃CN as solvent, containing 0.2 mol.dm⁻³ tetrabutylammonium hexafluorophosphate (TBAPF₆, [NBu₄][PF₆]) as supporting electrolyte. Measurements were conducted under a blanket of purified Argon. A three-electrode cell was used, consisting of a Pt auxiliary electrode, a glassy carbon working electrode (surface area 0.0707 cm²) and a Pt reference electrode [13,14]. The working electrode was polished first by a 3 μ m, followed by 1 μ m Diapat diamond paste on an abrasive cloth (in a figure-of-eight motion), rinsed with EtOH, H₂O and CH₃CN, and dried before each experiment. Scan rates varied between 0.050 and 5.000 V.s⁻¹. All experimental potentials were referenced against the redox couple of ferrocene (FcH) (IUPAC [15]). Either ferrocene or decamethyl ferrocene (Fc*, -0.508 V vs FcH/FcH⁺) was used as internal standard. Under these experimental conditions, ferrocene (FcH) exhibited a peak separation of $\Delta E_p = E_{pa} - E_{pc} = 0.069$ V and ratio $i_{pc}/i_{pa} = 1.00$; where E_{pa} (or E_{pc}) is the anodic (or cathodic) peak potential, and i_{pa} (or i_{pc}) is the anodic (or cathodic) peak current.

2.4 DFT calculations

Density functional theory (DFT) calculations were performed via the B3LYP functional (and UB3LYP for spin unrestricted calculations), as implemented in the Gaussian 09 package [16], using the triple- ζ basis set 6-311G(d,p) for the lighter atoms (C, H, N, O), whereas the Stuttgart/Dresden (SDD) pseudopotential was used to describe the Ru electronic core, while the metal valence electrons were described using the def2-TZVPP basis set [17]. Calculations were done in the gas phase, as well as the experimental solvent of the electrochemical study, CH₃CN with $\epsilon = 37.5$. The solvation model density (SMD) [18] polarizable continuum model (PCM) that was used, which solves the non-homogeneous Poisson equation by applying an integral equation formalism variant (IEF-PCM) [19].

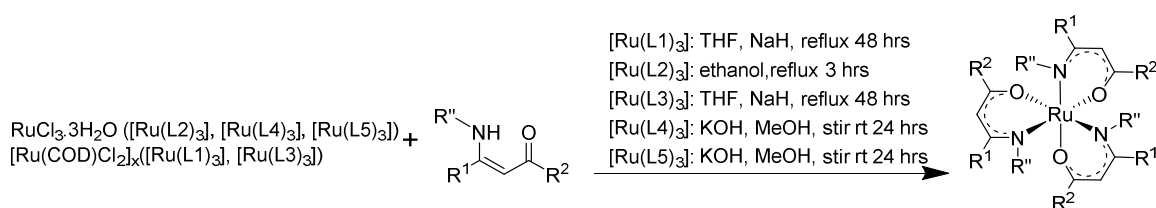
2.5 Mass Spectrometry

ESI-MS spectra (complexes **1**, **3**, **4**, **5**) (electrospray-ionization mass spectrometry) were collected on an ABSCIEX 4000QTRAP ion-trap mass spectrometer. The dried sample was dissolved in 1mL acetonitrile and further diluted 1000x before being infused into a Sciex 4000QTRAP hybrid triple quadrupole ion-trap mass spectrometer, at 10 μ L/min. During infusion a Q1 scan was performed between 100 and 800 Da in, while ramping the declustering potential between 0 and 400 V. The scan was performed in both positive and negative ionisation mode. The ionisation voltage was set at 5500V in positive mode and -4500V in negative mode, with a 10 psi curtain gas setting and 20 psi ionisation gas (GS1) setting.

MALDI-TOF-MS spectra (complex **2**) (matrix assisted laser desorption/ionization time-of-flight mass spectrometry) were collected by a Bruker Microflex LRF20 in the negative reflection mode, using the minimum laser power required to observe signals.

3 Results and Discussion

3.1 Synthesis



Scheme 2: Synthetic route for the tris(β -ketoiminato)ruthenium(III) complexes **1 – **5**. The ruthenium salt $[\text{Ru}(\text{COD})\text{Cl}_2]_2$ as used in the synthesis of complexes $[\text{Ru}(\text{L1})_3]$ and $[\text{Ru}(\text{L3})_3]$, while $\text{RuCl}_3 \cdot 3\text{H}_2\text{O}$ was used in the synthesis of complexes $[\text{Ru}(\text{L2})_3]$, $[\text{Ru}(\text{L4})_3]$ and $[\text{Ru}(\text{L5})_3]$, as shown on the left. The solvents and reaction conditions for each synthesis are shown on the right. The R^1 , R^2 and R'' groups are indicated in Scheme 1.**

The β -amino α,β -unsaturated ketoimine ligands **L1** – **L5** (**Scheme 1**), containing both N and O donor atoms, were synthesized as described in literature [10,11]. Scheme 2 indicates the general synthetic route for the preparation of the five tris(β -ketoiminato)ruthenium(III) complexes **1** – **5** of this study. Complexes **1** – **5** were prepared by either refluxing a mixture of a relevant ruthenium salt ($[\text{Ru}(\text{COD})\text{Cl}_2]_2 / \text{RuCl}_3 \cdot 3\text{H}_2\text{O}$) with the corresponding ketoimine ligands [12], or by stirring a mixture of $\text{RuCl}_3 \cdot 3\text{H}_2\text{O}$ and the relevant ketoimine ligand at room temperature [22]. The colour of each of the five complexes in the solid state appear black until dissolved in a solvent. When dissolved in a solvent, complexes $[\text{Ru}(\text{L1})_3]$ and $[\text{Ru}(\text{L2})_3]$ are dark blue, $[\text{Ru}(\text{L4})_3]$ appears green, $[\text{Ru}(\text{L5})_3]$ appears a very dark purple colour, while $[\text{Ru}(\text{L3})_3]$ appears brown. The complexes are stable in air, soluble in most organic solvents and are non-hygroscopic.

3.2 DFT results

3.2.1 Molecular Geometry

Both the *fac* and the *mer* isomers of all five synthesized tris(β -ketoiminato)ruthenium(III) complexes **1** – **5**, as well as the *mer* isomer only of complex **6** obtained from literature (Figure 1 with $\text{R}'' = \text{CH}_3$, $\text{R}^1 = \text{R}^2 = \text{CF}_3$), of which solid state crystal data was available from previous research [12], were optimized by DFT, with the resulting coordinates provided in the Supporting Information. Complex **6** is the available complex related to the complexes **1** – **5** of this study of which XRD data is available. Selected bond lengths and angles of the B3LYP density functional theory (DFT) optimized geometries of the six complexes studied, were summarized and compared with the existing XRD data of complex **6** [12] in Table 1. For complex **6**, the bonds involving ruthenium, Ru-N and Ru-O were accurately calculated within 0.03 Å of the provided experimental values. The O-Ru-N angles were calculated within 1.5° of the experimental values from literature; see Figure 1 for a root mean square (RMS) overlay of the calculated and experimental structures of complex **6**. The calculated bond lengths and angles for complex **6** were generally slightly larger than the experimental values, as often observed when comparing gas phase calculated structures with solid state experimental structures [20]. It was also observed that the calculated Ru-N and Ru-O bond lengths (and the O-Ru-N angles) of complexes **1** – **5** fall into a small range of 1.99-2.14 Å

(for Ru-N) and 1.99-2.08 Å (for Ru-O) (and 88-92° for O-Ru-N) respectively, with insignificant differences between the geometrical parameters of the *fac* and *mer* isomers. The three substituents R'', R¹ and R² on the β-ketoiminato ligands had little effect on the bond distance between the metal and the ligand.

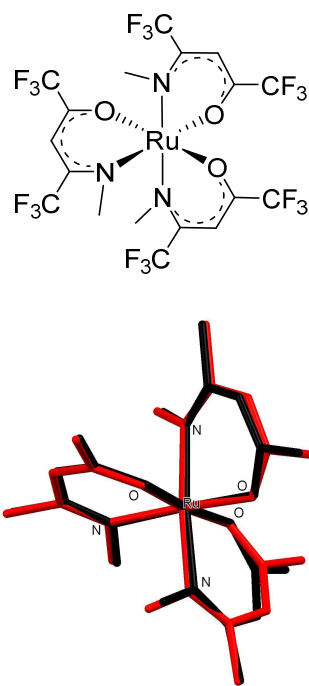


Figure 1: Top: Structure of [Ru(L6)₃] complex 6 (*mer* isomer) from literature, that was previously solved by XRD (CSD reference GAGROW [12]), (with the two ligand groups R¹ = R² = CF₃ and the group on the N donor atom R'' = CH₃). Bottom: RMS overlay (RMSD = 0.22) of the experimental (black) and B3LYP calculated (red) structure of complex 6 (H and F omitted for clarity).

Table 1: Selected bond lengths (Å) and bond angles (°) for the *mer* and *fac* isomers of complexes Ru(L1)₃ to Ru(L6)₃ as obtained from the theoretical B3LYP DFT calculations, as well as experimental crystallographic data only of the Ru(L6)₃ complex shown in Figure 1.

| | [Ru(L1) ₃] | | [Ru(L2) ₃] | | [Ru(L4) ₃] | | [Ru(L5) ₃] | | [Ru(L3) ₃] | | [Ru(L6) ₃] | | Exp <i>Mer</i> |
|----------|------------------------|------------|------------------------|------------|------------------------|------------|------------------------|------------|------------------------|------------|------------------------|------------|-------------------|
| | <i>Mer</i> | <i>Fac</i> | <i>Mer</i> | <i>Mer</i> | |
| Ru-N1 | 2.084 | 2.137 | 2.022 | 2.000 | 2.095 | 2.096 | 2.033 | 1.995 | 2.016 | 1.990 | 2.112 | 2.090 | |
| Ru-N2 | 2.125 | 2.102 | 2.031 | 2.016 | 2.121 | 2.107 | 2.019 | 2.028 | 2.027 | 2.015 | 2.063 | 2.037 | |
| Ru-N3 | 2.069 | 2.078 | 2.068 | 2.038 | 2.085 | 2.087 | 2.085 | 2.021 | 2.060 | 2.025 | 2.064 | 2.042 | |
| Ru-O1 | 2.039 | 2.026 | 2.045 | 2.042 | 2.036 | 2.057 | 2.061 | 2.040 | 2.044 | 2.038 | 2.014 | 2.015 | |
| Ru-O2 | 2.046 | 2.043 | 2.020 | 2.078 | 2.030 | 2.019 | 2.044 | 2.036 | 2.012 | 2.078 | 2.001 | 1.984 | |
| Ru-O3 | 2.012 | 2.029 | 2.024 | 2.040 | 2.010 | 2.029 | 2.019 | 2.078 | 2.018 | 2.034 | 2.020 | 2.013 | |
| O1-Ru-N1 | 89.4 | 92.0 | 90.0 | 91.1 | 90.7 | 89.7 | 90.1 | 90.9 | 89.9 | 90.8 | 90.6 | 92.1 | |
| O2-Ru-N2 | 90.8 | 89.4 | 88.2 | 88.5 | 91.0 | 89.6 | 89.0 | 87.9 | 88.9 | 87.7 | 91.1 | 91.7 | |
| O3-Ru-N3 | 90.6 | 89.5 | 88.9 | 87.8 | 90.3 | 92.1 | 88.1 | 88.5 | 87.8 | 88.3 | 91.1 | 90.7 | |

3.2.2 Energy

Results obtained in the previous section showed that the B3LYP DFT method provided a reliable calculated structure for complexes **1** – **5**, when compared to existing experimental crystallographic data from a similar compound (**6** obtained from literature). In order to determine whether the electronic energy of these complexes also was accurate, the possible spin states, $S = 1/2, 3/2$ and $5/2$, were calculated for the d^5 complex **2** using two different functionals, see Table 2. The results were in agreement with experimental observation [21,22], clearly showing that the neutral tris(β -ketoiminato)ruthenium(III) complexes **1** – **5** of this study were all low-spin with $S = 1/2$.

Table 2: Relative electronic energy (eV) for complex Ru(L2)₃, calculated by the different DFT functionals, as indicated. Lowest energies are indicated in bold font.

| Isomer | S | ΔE (eV) | | |
|------------|-----|-----------------|-------------|-------------|
| | | B3LYP | B3LYP-D3 | OLYP |
| <i>fac</i> | 1/2 | 0.02 | 0.00 | 0.00 |
| | 3/2 | 1.93 | 2.38 | 1.70 |
| | 5/2 | 3.27 | 3.80 | 2.85 |
| <i>mer</i> | 1/2 | 0.00 | 0.06 | 0.01 |
| | 3/2 | 1.59 | 2.07 | 1.41 |
| | 5/2 | 3.09 | 3.65 | 2.71 |

The relative energies and populations according to the Boltzmann equation of the *fac* and *mer* isomers of complexes **1** – **6** were listed in Table 3. The results showed that for complexes **2**, **3** and **5** (Series 1, with $R'' = H$), both the *fac* and *mer* isomer could exist, with *fac* the main isomer in solution. However, for complexes **1** and **4** (Series 2, with $R'' = Ph$), as well as complex **6** from literature (with $R'' = CH_3$), the *mer* isomer was favoured. The *mer* isomers of the latter were less affected by steric hindrance caused by the Ph or CH_3 groups (on the N donor atom of each ligands), when compared to their *fac* isomers; see Figure 2. This result was also in agreement with the fact that only the *mer* isomer of complex **6** was isolated in the solid state [12].

Table 3: Relative energies (eV) and population (%) for complexes 1 – 6 in the two ligand series, obtained from theoretical DFT calculations in both the gas and solvent phase, using CH₃CN as solvent.

| | Gas phase | | Gas phase | | Solvent (CH ₃ CN) | | Solvent (CH ₃ CN) | |
|---|------------------|--------|------------------|--------|------------------------------|--------|------------------------------|-------|
| | B3LYP | | B3LYP-D3 | | B3LYP | | B3LYP-D3 | |
| | E _{rel} | % | E _{rel} | % | E _{rel} | % | E _{rel} | % |
| Series 1 with R'' = H | | | | | | | | |
| [Ru(L2) ₃] - <i>fac</i> | 0.02 | 32.71 | 0.02 | 33.85 | 0.00 | 90.81 | 0.00 | 90.13 |
| [Ru(L2) ₃] - <i>mer</i> | 0.00 | 67.29 | 0.00 | 66.15 | 0.06 | 9.19 | 0.06 | 9.87 |
| [Ru(L5) ₃] - <i>fac</i> | 0.00 | 50.55 | 0.01 | 43.14 | 0.00 | 90.82 | 0.00 | 83.67 |
| [Ru(L5) ₃] - <i>mer</i> | 0.00 | 49.45 | 0.00 | 56.86 | 0.06 | 9.18 | 0.04 | 16.33 |
| [Ru(L3) ₃] - <i>fac</i> | 0.00 | 78.33 | 0.00 | 83.44 | 0.00 | 96.69 | 0.00 | 96.50 |
| [Ru(L3) ₃] - <i>mer</i> | 0.03 | 21.67 | 0.04 | 16.56 | 0.09 | 3.31 | 0.09 | 3.50 |
| Series 2 with R'' = Ph or CH₃ | | | | | | | | |
| [Ru(L1) ₃] - <i>fac</i> | 0.23 | 0.01 | 0.12 | 0.88 | 0.21 | 0.03 | 0.09 | 2.74 |
| [Ru(L1) ₃] - <i>mer</i> | 0.00 | 99.99 | 0.00 | 99.12 | 0.00 | 99.97 | 0.00 | 97.26 |
| [Ru(L4) ₃] - <i>fac</i> | 0.19 | 0.07 | 0.22 | 0.02 | 0.19 | 0.05 | 0.21 | 0.03 |
| [Ru(L4) ₃] - <i>mer</i> | 0.00 | 99.93 | 0.00 | 99.98 | 0.00 | 99.95 | 0.00 | 99.97 |
| [Ru(L6) ₃] - <i>fac</i> | 0.29 | 0.00 | 0.35 | 0.00 | 0.20 | 0.00 | 0.24 | 0.01 |
| [Ru(L6) ₃] - <i>mer</i> | 0.00 | 100.00 | 0.00 | 100.00 | 0.00 | 100.00 | 0.00 | 99.99 |

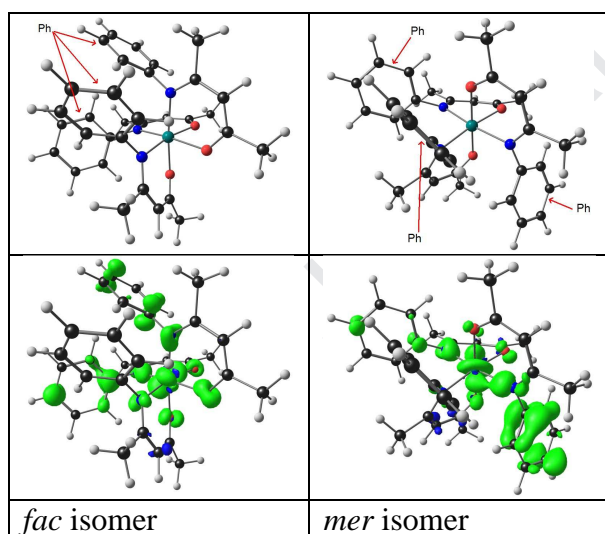


Figure 2: Top: B3LYP geometry of the *fac* (left) and *mer* (right) isomer of complex 1, highlighting the higher steric hindrance caused by the Ph group (on the N donor atom of each ligand) in the *fac* isomer (top left) than in the *mer* isomer. Bottom: Spin density plot of the *fac* (left) and *mer* (right) isomer of complex 1. Contour = 0.004 eÅ⁻³.

3.2.3 Electronic structure

Selected frontier molecular orbitals of complex 2 were shown in Figure 3. The neutral d⁵ Ru(III)-complex 2 with S = ½ has three alpha and two beta Ru-d based molecular orbitals (MOs).

Both the highest occupied molecular orbital (HOMO) and the lowest unoccupied molecular orbital (LUMO) of complex **2** were of Ru-d character, while the LUMO+1 was β -ketoiminato ligand based (see Figure 4). The spin density plot of complexes **1** – **5** showed the locus of the unpaired electron on each complex. The spin distribution indicated that about $0.80 e^-$ was distributed over the Ru-metal for all the complexes, with the rest of the electron density distributed over both donor atoms (N and O) and the central carbon between (C-N) and (C-O) on the β -ketoiminato ligands (see Table S1 and Figure S3). For the complexes of Series 2 where $R'' = \text{Ph}$ (namely $[\text{Ru}(\text{L1})_3]$ and $[\text{Ru}(\text{L4})_3]$), the spin was additionally distributed over two of the three Ph groups on the R'' positions on the N donor atom (Figure S3). The Mulliken spin population on Ru of *ca.* 0.8 was nearing value 1 (Table S1), which is consistent with a low-spin Ru(III) centre.

During the reduction of the neutral Ru(III) complex, an electron is added to the complex. This added electron could either go into the β -LUMO resulting in $q = -1$ and $S = 0$, or into the α -LUMO (overall LUMO+1), resulting in two unpaired electrons for the reduced complex with $q = -1$ and spin = 1. DFT calculations for **2** showed that the complex with spin = 0 had a lower energy compared to the complex with spin = 1 (with $\Delta E = 1 - 1.5$ eV for complexes **1** – **5**), therefore the electron added upon reduction of complex **2** was added to the β -LUMO. Since the β -LUMO is Ru-d based, the first reduction of complex **2** was therefore proven to be metal based, i.e. $\text{Ru}^{\text{III/II}}$ reduction.

In contrast, during oxidation, an electron is removed from the molecule. This electron could either be removed from the β -HOMO, resulting in $q = 1$ and spin = 1, or from the α -HOMO (overall HOMO-1) resulting in $q = 1$ and spin = 0 (no unpaired electrons). DFT calculations for **1** - **5** showed that the complex with spin = 1 had the lowest energy compared to the complex with spin = 0, with $\Delta E = 0.2 - 0.3$ eV, implying that the reduced complex was diamagnetic with $S = 0$. Since the β -HOMO is Ru-d based, the first oxidation of complex **2** was therefore proven to be metal based, i.e. $\text{Ru}^{\text{III/IV}}$ oxidation.

A second reduction would involve an added electron, either to the LUMO+1 of the neutral complex, or to the LUMO of the reduced complex. These MOs did not have Ru-d character and were ligand based, see Figure 4. Thus the second reduction of complex **2** was proven to be ligand based.

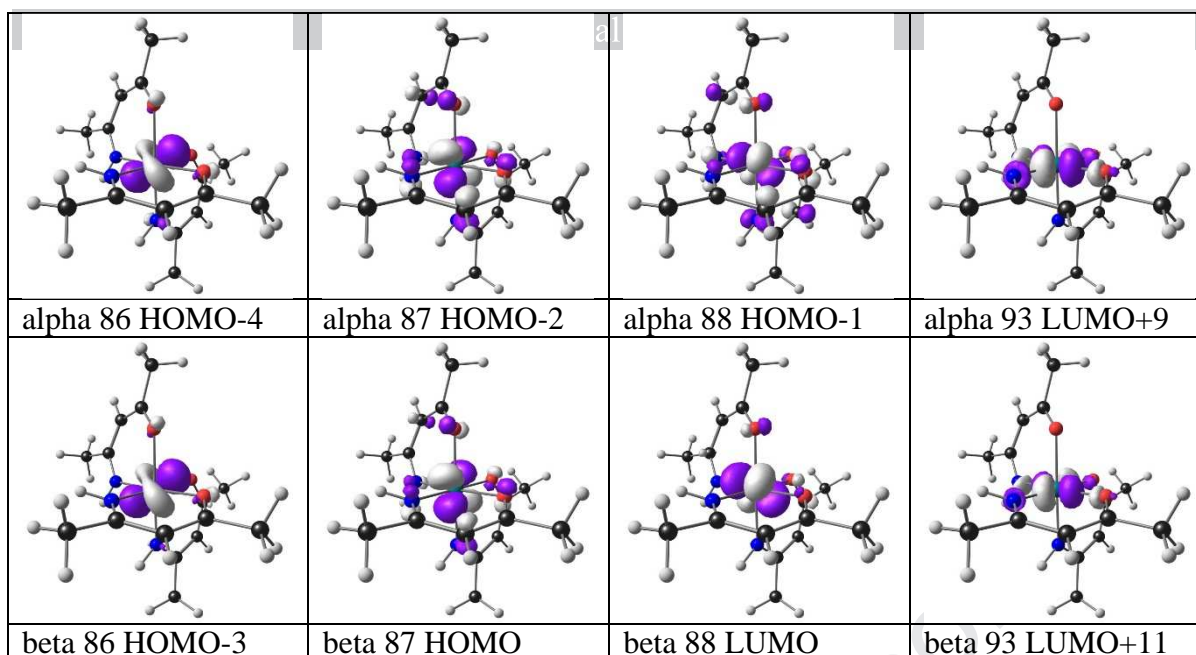


Figure 3: Selected B3LYP calculated MOs of the *fac* isomer of the tris(β -ketoiminato)ruthenium(III) complex **2** of this study. The contour used for the MO plots is $0.08 \text{ e}\text{\AA}^{-3}$.

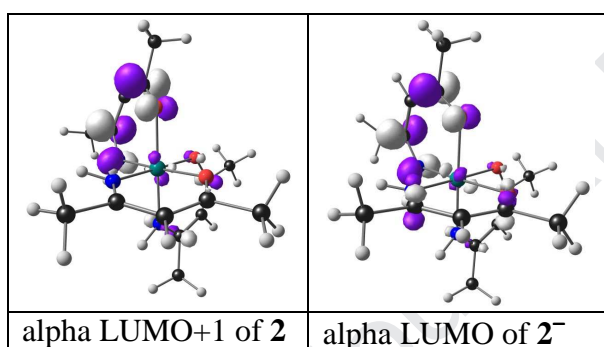


Figure 4: B3LYP calculated LUMO+1 of the *fac* isomer of complex **2** and LUMO of the anion of **2**. The contour used for the MO plots is $0.07 \text{ e}\text{\AA}^{-3}$.

Similarly to complex **2**, the LUMO and the HOMO of complexes **1**, **3** – **5** were also proven to be predominantly Ru-d based, however extending further by small amounts also to the two donor atoms N and O, as well as to the central carbon between (C-N) and (C=O) on the ligand (see Figure S1).

Table 4 shows both the HOMO and LUMO energies for the *mer* and *fac* isomers of complexes **1** – **5**. The results in Table 4 showed that in all five complexes both HOMO and LUMO energies of the *fac* isomer were lower (more negative) than those of the *mer* isomer, except for complex $[\text{Ru}(\text{L}3)_3]$ B3LYP-D3 gas phase calculations where the order reversed, though the gas phase energies of the HOMOs of the two isomers differ only with only 0.003 eV. This means that the *fac* isomer was reduced more readily than the *mer* isomer (since it is easier to accept an electron in a

lower energy LUMO). The *mer* isomer, however, was oxidized more easily than the *fac* isomer, since it is easier to remove an electron from a higher energy HOMO.

Journal Pre-proof

Table 4: DFT calculated HOMO and LUMO energies (eV) for the two possible isomers *fac* and *mer* of the five Ru(III) complexes 1 – 5 in the two ligand series.

| | Gas | | Gas | | Solvent (CH ₃ CN) | | Solvent (CH ₃ CN) | |
|-------------------------------------|------------------------|------------------------|------------------------|------------------------|------------------------------|------------------------|------------------------------|------------------------|
| | B3LYP | | B3LYP-D3 | | B3LYP | | B3LYP-D3 | |
| | E _{HOMO} (eV) | E _{LUMO} (eV) | E _{HOMO} (eV) | E _{LUMO} (eV) | E _{HOMO} (eV) | E _{HOMO} (eV) | E _{HOMO} (eV) | E _{HOMO} (eV) |
| Series 1 with R'' = H | | | | | | | | |
| [Ru(L2) ₃] - <i>fac</i> | -4.703 | -2.219 | -4.721 | -2.179 | -5.064 | -2.604 | -5.074 | -2.559 |
| [Ru(L2) ₃] - <i>mer</i> | -4.666 | -2.173 | -4.670 | -2.137 | -5.049 | -2.552 | -5.049 | -2.506 |
| [Ru(L5) ₃] - <i>fac</i> | -4.827 | -2.412 | -4.840 | -2.343 | -5.152 | -2.751 | -5.157 | -2.695 |
| [Ru(L5) ₃] - <i>mer</i> | -4.812 | -2.387 | -4.813 | -2.327 | -5.137 | -2.704 | -5.137 | -2.638 |
| [Ru(L3) ₃] - <i>fac</i> | -4.897 | -2.529 | -4.898 | -2.463 | -5.245 | -2.911 | -5.223 | -2.845 |
| [Ru(L3) ₃] - <i>mer</i> | -4.860 | -2.515 | -4.840 | -2.466 | -5.224 | -2.864 | -5.183 | -2.811 |
| Series 2 with R'' = Ph | | | | | | | | |
| [Ru(L1) ₃] - <i>fac</i> | -4.876 | -2.516 | -4.843 | -2.541 | -5.216 | -2.849 | -5.167 | -2.866 |
| [Ru(L1) ₃] - <i>mer</i> | -4.784 | -2.379 | -4.747 | -2.362 | -5.105 | -2.681 | -5.041 | -2.635 |
| [Ru(L4) ₃] - <i>fac</i> | -4.964 | -2.630 | -4.922 | -2.635 | -5.283 | -2.953 | -5.229 | -2.952 |
| [Ru(L4) ₃] - <i>mer</i> | -4.899 | -2.524 | -4.831 | -2.475 | -5.195 | -2.816 | -5.105 | -2.733 |

3.3 CV results

The redox behaviour of the five ruthenium(III) complexes **1** – **5** in this research were studied under the conditions discussed in section 2.3. Selected electrochemical data was summarized in Table 5, and representative voltammograms were shown in Figure 5 (for Series 1) and Figure 6 (for Series 2). All five these complexes showed two to three redox couples in the solvent window possible for CH₃CN. The first redox couple on the anodic side, and the first redox couple on the cathodic side, were assigned respectively to the oxidation of Ru(III) to Ru(IV), and the reduction of Ru(III) to Ru(II). This assignment was in agreement with the DFT study presented in Section 3.2.3, and also in qualitative agreement with the redox behaviour of a related tris(β -diketonato)ruthenium(III) complex [Ru(acac)₃] from literature [²³], that also exhibited a Ru(III)/(IV) oxidation on the anodic side, and a Ru(III)/(II) reduction on the cathodic side. For complexes **3**, **4** and **5** a second redox process was observed below 1.9 V vs FcH/FcH⁺; see Figure 6 for complex **4** as an example. This second redox process was assigned to the reduction of the coordinated β -ketoimine ligands of the tris(β -ketoiminato)ruthenium(III) complexes of this study (see section 3.2.3 and Figure 4). This ligand based reduction of complexes **1** and **2** was not observed in the solvent window possible for CH₃CN.

The Ru(III)/(IV) oxidation on the anodic side, between -0.04 to 0.70 V vs FcH/FcH⁺, consisted of two oxidation peaks with two associated reduction peaks, which were assigned in accordance to the DFT results presented in Section 3.2.3 above, namely as the oxidation of firstly the *mer* isomer and secondly the *fac* isomer of each complex. The first Ru(III)/(IV) redox couple, which was assigned to the *mer* isomer, was reversible with $\Delta E_p = 0.061 - 0.079$ V, while for the second oxidation wave which was associated with the *fac* isomer, the ΔE_p value was between 0.061 - 0.077 V. The Ru(III)/(IV) oxidation occurred at the potential range of -0.04 V to 0.40 V for the *mer* isomers, and at 0.12 V to 0.67 V for the *fac* isomers. It was observed that the Ru(III)/(IV) oxidation occurred at increasingly higher oxidation potentials, as the amount of aromatic Ph groups at the R¹ and R² position increased from 0 (complex **2**) to 1 (complex **5**) to two Ph groups (complex **3**) in the Series 1 complexes; see Figure 5. The same trend was observed for the Series 2 complexes, when comparing complex **1** (no Ph group at R¹ or R²) with complex **4** (one Ph group at R²); see Figure 6.

The Ru(III)/(II) reduction on the cathodic side between -1.52 V to -0.89 V vs FcH/FcH⁺, showed a different behaviour for the different complexes. For Series 1 complexes (Figure 5), the following was obtained: Complex **2** showed one reversible Ru(III)/(II) redox couple between -

1.358 V and -1.426 V (with $\Delta E_p = 0.068$ V), which was assigned to the reduction of the closely overlapping *fac* and *mer* isomers of complex **2**. Complex **5** on the other hand showed two Ru(III)/(II) redox couples between -1.232 V and -1.006 V, which were assigned to the reduction of the *fac* and the *mer* isomer of **5** respectively. Complex **3** again showed one Ru(III)/(II) redox couple between -0.864 V and -0.925 V (with $\Delta E_p = 0.061$ V), which also was assigned to the reduction of the closely overlapping *fac* and *mer* isomers of **3**.

For the Series 2 complexes (Figure 6), a very small reduction peak was obtained at -1.243 V for the *fac* isomer of complex **1**, and a larger reduction peak at -1.552 V (with the corresponding oxidation peak at -1.486 V) for the *mer* isomer of complex **1**. The observed small reduction peak for the *fac* isomer was consistent with the DFT study above, which showed that due to steric hindrance, complex **1** existed mainly in the *mer* form. For complex **4** also of Series 2, the reversible ($\Delta E_p = 0.067$ V) reduction wave between -1.437 V and -1.370 V, was assigned to the reduction of the *fac* and *mer* isomer closely overlapping. Only one Ru(III)/(II) reduction peak was observed for complex **4**, at all scan rates from 0.05 up to 5.00 V s⁻¹; see Figure S5.

The *fac-mer* equilibrium observed here thus seemed to be slow and did not change with time or scan rate. The experimental assignment of redox peaks of the different isomers was previously made possible by observance of the slow *fac-mer* and keto-enol equilibrium kinetics of related chromium-carbene complexes [24] and ruthenocene-containing β -diketones [25] respectively. For the *fac* and *mer* isomers of the chromium-carbene complexes, different peaks *ca.* 0.2 V apart, were observed for the oxidation of the *fac* and *mer* isomers, similarly to the difference between the *fac* and *mer* oxidation observed for **1** – **5**. For some chromium-carbene complexes, the reduction of both *fac* and *mer* isomers could be distinguished, while for other chromium-carbene complexes only one reduction peak was observed, since in the latter case the reduction peaks of the *fac* and *mer* isomers were too near to each other to be distinguished [25]. This is similar to the redox behaviour that was obtained here for complexes **1** and **5** (two reduction peaks for the *fac* and *mer* isomers respectively) and for complexes **2**, **3** and **4** (one reduction peak only for both the *fac* and *mer* isomer, closely overlapping).

The same trend that was observed for the Ru(III)/(IV) oxidation, was also observed for the Ru(III)/(II) reduction, namely that the reduction occurred at an increasingly higher potential, as the amount of aromatic Ph groups at the R¹ and R² positions increased from 0 (complex **2**) to 1 (complex **5**) to two Ph groups (complex **3**) in the Series 1 complexes (Figure 5). Similarly, the reduction also occurred at an increasingly higher potential, as the amount of aromatic Ph groups at the R¹ and R² positions increased from 0 (complex **4**) to 1 Ph group (complex **1**) in the Series 1 complexes (Figure 6).

The potential difference between the two successive redox processes (Ru(III)/Ru(II) and Ru(III)/Ru(IV)) of complexes **1** – **5**, was 1.3 V to 1.6 V. This result was in line with previous studies of Ru(III) complexes, which showed that the average potential difference between two successive redox processes (Ru(III)/Ru(II) and Ru(III)/Ru(IV)) was 1.2 V to 1.7 V [26,27].

It was further observed that both the Ru(III)/Ru(II) reduction and the Ru(III)/Ru(IV) oxidation of complexes **1** and **2** (containing N,O-bidentate ligands of the type $(\text{CH}_3\text{C}(\text{NR}'')\text{CHCOCH}_3)^-$), occurred at a lower potential than the Ru(III)/Ru(II) reduction ($-1.15 \text{ V vs Fc/Fc}^+$) and the Ru(III)/Ru(IV) oxidation ($0.602 \text{ V vs Fc/Fc}^+$) of the related $[\text{Rh}(\text{acac})_3]$ compound from literature (containing the O,O-bidentate ligand acac = acetylacetonato = $(\text{CH}_3\text{COCHCOCH}_3)^-$) [23]. This observation also agrees with literature results obtained for $[\text{Ru}(\text{O},\text{O-BID})_{3-n}(\text{N},\text{O-BID})_n]$ ($n = 1$ or 2), where it was observed that when one of the two O,O bidentate ligands was substituted with a N,O bidentate ligand from $[\text{Ru}(\text{acac})_3]$ (acac = acetylacetonato = $(\text{CH}_3\text{COCHCOCH}_3)^-$), both the Ru(III)/Ru(II) reduction and the Ru(III)/Ru(IV) oxidation occurred at a lower potential [22].

Table 5: The summary of the cyclic voltammetric data of the Ru(III) complexes.

| | Oxidation Ru(III)/(IV) | | | | Reduction Ru(III)/(II) | | | |
|----------------------------------|------------------------|----------|------------|----------|------------------------|----------|------------|----------|
| | E_{pc} | E_{pa} | ΔE | $E^{0'}$ | E_{pc} | E_{pa} | ΔE | $E^{0'}$ |
| Series 1 | | | | | | | | |
| $[\text{Ru}(\text{L2})_3] - fac$ | 0.082 | 0.159 | 0.077 | 0.121 | -1.426 | -1.358 | 0.068 | -1.392 |
| $[\text{Ru}(\text{L2})_3] - mer$ | -0.078 | -0.003 | 0.075 | -0.041 | | | | |
| $[\text{Ru}(\text{L3})_3] - fac$ | 0.641 | 0.703 | 0.062 | 0.672 | -0.925 | -0.864 | 0.061 | -0.895 |
| $[\text{Ru}(\text{L3})_3] - mer$ | 0.369 | 0.430 | 0.061 | 0.400 | | | | |
| $[\text{Ru}(\text{L5})_3] - fac$ | 0.363 | 0.426 | 0.063 | 0.395 | -1.069 | -1.006 | 0.063 | -1.038 |
| $[\text{Ru}(\text{L5})_3] - mer$ | 0.144 | 0.206 | 0.062 | 0.175 | -1.232 | -1.165 | 0.067 | -1.199 |
| Series 2 | | | | | | | | |
| $[\text{Ru}(\text{L1})_3] - fac$ | 0.215 | 0.276 | 0.061 | 0.246 | -1.243 | -1.172 | 0.071 | -1.208 |
| $[\text{Ru}(\text{L1})_3] - mer$ | 0.032 | 0.097 | 0.065 | 0.065 | -1.552 | -1.486 | 0.066 | -1.519 |
| $[\text{Ru}(\text{L4})_3] - fac$ | - | 0.508 | | | -1.437 | -1.370 | 0.067 | -1.404 |
| $[\text{Ru}(\text{L4})_3] - mer$ | 0.058 | 0.137 | 0.079 | 0.098 | | | | |

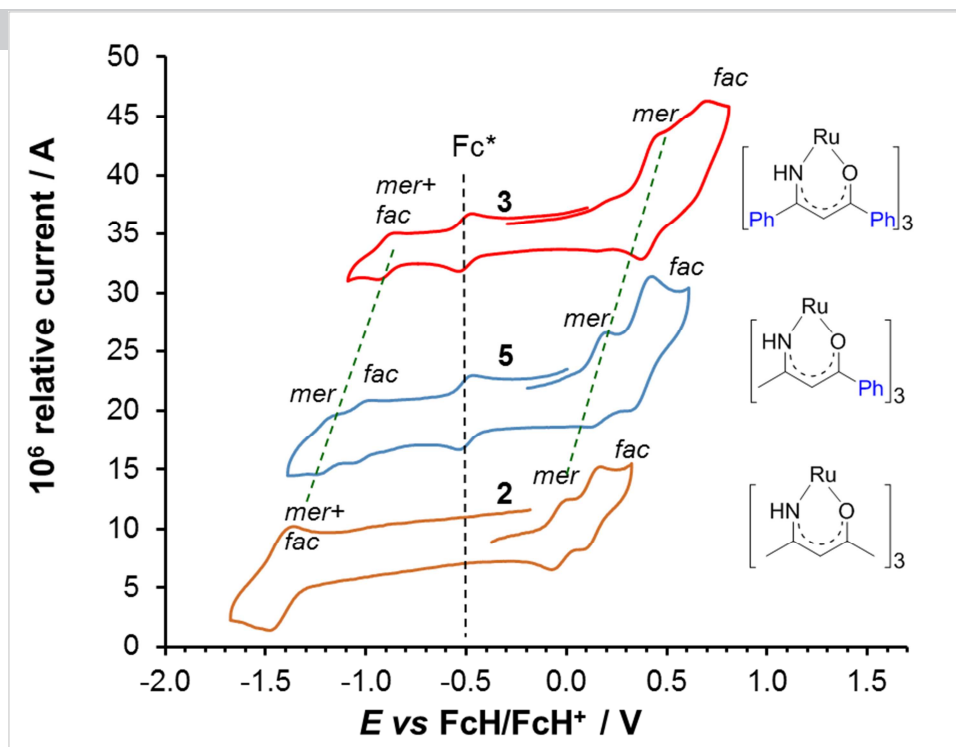


Figure 5: Cyclic voltammograms (versus FcH/FcH^+) of Series 1, tris(β -ketoiminato)ruthenium(III) complexes 2, 5 and 3 of this study, at a scan rate of 0.100 V s^{-1} . Decamethyl ferrocene (Fc^*) was used as internal standard reference. Scans were initiated from *ca.* -0.3 V in the positive direction. The CVs were measured in 0.2 mol dm^{-3} $\text{TBAPF}_6/\text{CH}_3\text{CN}$, on a glassy carbon working electrode at $25 \text{ }^\circ\text{C}$.

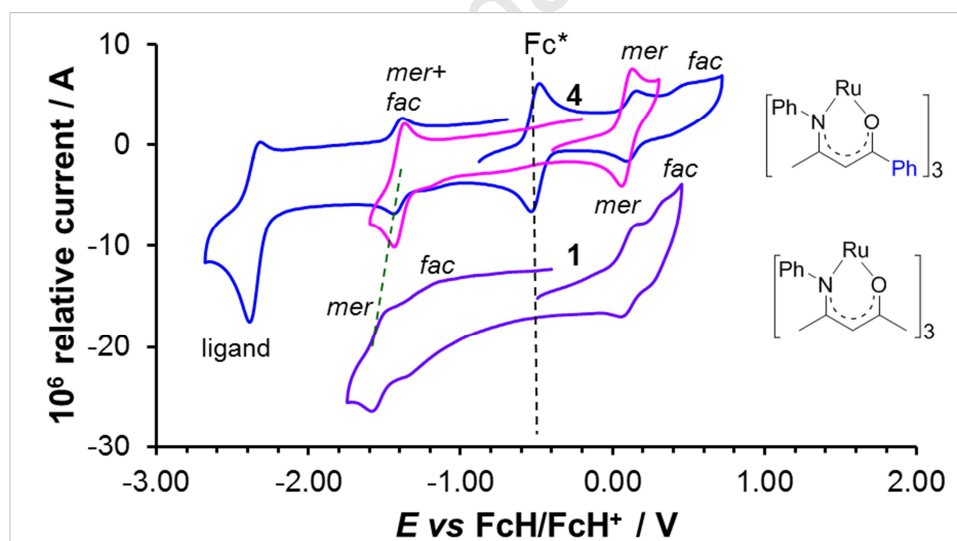


Figure 6: Cyclic voltammograms (versus FcH/FcH^+) of Series 2, of tris(β -ketoiminato)ruthenium(III) complexes 1 and 4 of this study, at a scan rate of 0.100 V s^{-1} . Decamethyl ferrocene (Fc^*) was used as internal standard reference. Scans were initiated from *ca.* -0.3 V in the positive direction. The CVs were measured in 0.2 mol dm^{-3} $\text{TBAPF}_6/\text{CH}_3\text{CN}$, on a glassy carbon working electrode at $25 \text{ }^\circ\text{C}$.

The DFT calculations showed that tris(β -ketoiminato)ruthenium(III) complexes **2**, **5** and **3** mainly favour the *fac* isomer, while complexes **1** and **4** favour the *mer* isomer in solution, due to steric hindrance of the Ph group on the R'' position. Moreover, the spin density plots of complexes **1** – **5** showed that 80% of the electron distribution was distributed over the metal, while the rest was distributed over the donor atoms N and O, spreading over the central carbon between (C-N) and (C-O) on the β -ketoiminato ligand. DFT calculations also showed that the first reduction and the first oxidation was Rh-d-metal based. Electrochemistry results showed that oxidation of Ru(III) to Ru(IV) occurred between -0.04 V to 0.70 V vs FcH/FcH⁺, and reduction of Ru(III) to Ru(II) between -0.90 V to -1.52 V vs FcH/FcH⁺. The experimental results also showed that two oxidation peaks occurred, due to the two isomers, *mer* and *fac*. The DFT results showed that the *mer* isomer will be oxidised first, while the *fac* isomer will be reduced first. Lastly, the experimental results (Cyclic Voltammetry) showed that both the oxidation (Ru(III) to Ru(IV)) and reduction (Ru(III) to Ru(II)) potentials increased with an increase in the amount of aromatic Ph groups at the R¹ and R² positions, for both ligand series 1 and 2.

Acknowledgements

This work has received support from the South African National Research Foundation (Grant Nos: 113327 and 96111) and the Central Research Fund of the University of the Free State, Bloemfontein. The High Performance Computing facility of the UFS is acknowledged for computer time.

Supporting Information

Optimized coordinates of the DFT calculations, additional figures and tables.

References

[¹] S.J. Lucas, R.M. Lord, R.L. Wilson, R.M. Phillips, V. Sridharana and P.C. McGowan, Synthesis of iridium and ruthenium complexes with (N,N), (N,O) and (O,O) coordinating bidentate ligands as

potential anti-cancer agents, Dalton Trans. 41 (2012) 13800-13802, <https://doi.org/10.1039/C2DT32104A>

[²] J. Wang, Y. Zhao, X. Jin, L. Yang, H. Wang, Structural, electronic, vibrational and NMR spectral analyses of [Ru(OAc)(2cqn)₂NO] (H₂cqn = 2-chloro-8-quinolinol) isomers, Spectrochim. Acta Part A: Molecular and Biomolecular Spectroscopy 122 (2014) 649–655, <https://doi.org/10.1016/j.saa.2013.11.105>

[³] A.F. Shoair, A.A. El-Bindary, Synthesis, spectral and catalytic dehydrogenation studies of ruthenium complexes containing NO bidentate ligands, Spectrochim. Acta Part A: Molecular and Biomolecular Spectroscopy 131 (2014) 490–496, <https://doi.org/10.1016/j.saa.2014.04.132>

[⁴] P.P. Lainé, S. Campagna, F. Loiseau, Conformationally gated photoinduced processes within photosensitizer–acceptor dyads based on ruthenium(II) and osmium(II) polypyridyl complexes with an appended pyridinium group, Coord. Chem. Rev. 252 (2008) 2552–2571, <https://doi.org/10.1016/j.ccr.2008.05.007>

[⁵] C.-C. Chou, K.-L. Wu, Y. Chi, W.-P. Hu, S.J. Yu, G.-H. Lee, C.-L. Lin, P.-T. Chou, Ruthenium(II) Sensitizers with Heteroleptic Tridentate Chelates for Dye-Sensitized Solar Cells, Angew. Chem. Int. Ed. 50 (2011) 2054–2058, <https://doi.org/10.1002/anie.201006629>

[⁶] E.U. Barın, M. Masjedi, S. Özkar, A New Homogeneous Catalyst for the Dehydrogenation of Dimethylamine Borane Starting with Ruthenium(III) Acetylacetonate, Materials 8 (2015) 3155–3167, <https://doi.org/10.3390/ma8063155>;

R. Varala, S.R. Adapa, Ruthenium(III) acetylacetonate [Ru(acac)₃] — An efficient chemoselective catalyst for the tetrahydropyranylation (THP) of alcohols and phenols under solvent-free conditions, Can. J. Chem. 84 (2006) 1174 – 1179, <https://doi.org/10.1139/v06-137>;

R. Varala, A. Nasreen, S.R. Adapa, Ruthenium(III) acetylacetonate [Ru(acac)₃] — An efficient recyclable catalyst for the acetylation of phenols, alcohols, and amines under neat conditions, Can. J. Chem. 85 (2007) 148-152, <https://doi.org/10.1139/v06-191>;

H.T. Teunissen, C.J. Elsevier, Ruthenium catalysed hydrogenation of dimethyl oxalate to ethylene glycol, Chem. Commun. (1997) 667-668, <http://dx.doi.org/10.1039/A700862G>

[⁷] J.F. Kucharyson, J.R. Gaudet, B.M. Wyvrat, L.T. Thompson, Characterization of Structural and Electronic Transitions During Reduction and Oxidation of Ru(acac)₃ Flow Battery Electrolytes by using X-ray Absorption Spectroscopy, Chem. Electro. Chem. 3 (2016) 1875-1883. <https://doi.org/10.1002/celec.201600360>

[⁸] D. Wang, D Astruc, The recent development of efficient Earth-abundant transition-metal nanocatalysts, Chem. Soc. Rev. 46 (2017) 816-854, <https://doi.org/10.1039/c6cs00629a>

- [⁹] M.J. Sarsfield, I. May, S.M. Cornet, M. Helliwell, Preference for Nitrogen versus Oxygen Donor Coordination in Uranyl and Neptunyl(VI) Complexes, *Inorg. Chem.* 44:21 (2005) 7310-7312, <https://doi.org/10.1021/ic051161c>
- [¹⁰] M.E.F. Braibante, H.S. Braibante, L. Missio, A. Andricopulo, Synthesis and reactivity of β -amino α,β -unsaturated ketones and esters using K-10 montmorillonite, *Synthesis* 1994:9 (1994) 898-900, <http://dx.doi.org/10.1055/s-1994-25595>
- [¹¹] T.L. Ngake, J.H. Potgieter, J. Conradie, Electrochemical behaviour of amino substituted β -amino α,β unsaturated ketones: A computational chemistry and experimental study. *Electrochim. Acta* 296 (2019) 1070-1082, <https://doi.org/10.1016/j.electacta.2018.11.144>
- [¹²] T.-Y. Chou, Y.-H. Lai, Y.-L. Chen, Y. Chi, K.R. Prasad, A.J. Carty, S.-M. Peng, G.-H. Lee, Synthesis and Characterization of tris(β -ketoiminato)ruthenium(III) complexes: Potential Precursors for CVD of Ru and RuO₂ Thin Films, *Chem. Vap. Deposition* 10 (2004) 149-158, <https://doi.org/10.1002/cvde.200306284>
- [¹³] D.T. Sawyer, J.L. Roberts (Jr.), *Experimental Electrochemistry for Chemists*, John Wiley & Sons, New York, 1974, p. 54.
- [¹⁴] D.H. Evans, K.M. O'Connell, R.A. Peterson, M.J. Kelly, Cyclic Voltammetry, *J. Chem. Ed.* 60:4 (1983) 290-293, <http://dx.doi.org/10.1021/ed060p290>
- [¹⁵] G. Gritzner, J. Kuta, Recommendations on reporting electrode potentials in nonaqueous solvents, *Pure and Applied Chemistry* 56:4 (1984) 461-466
- [¹⁶] M.J. Frisch, G.W. Trucks, H.B. Schlegel, G.E. Scuseria, M.A. Robb, J.R. Cheeseman, G. Scalmani, V. Barone, B. Mennucci, G.A. Petersson, H. Nakatsuji, M. Caricato, X. Li, H.P. Hratchian, A.F. Izmaylov, J. Bloino, G. Zheng, J.L. Sonnenberg, M. Hada, M. Ehara, K. Toyota, R. Fukuda, J. Hasegawa, M. Ishida, T. Nakajima, Y. Honda, O. Kitao, H. Nakai, T. Vreven, J.A. Montgomery (Jr.), J.E. Peralta, F. Ogliaro, M. Bearpark, J.J. Heyd, E. Brothers, K.N. Kudin, V.N. Staroverov, R. Kobayashi, J. Normand, K. Raghavachari, A. Rendell, J.C. Burant, S.S. Iyengar, J. Tomasi, M. Cossi, N. Rega, J.M. Millam, M. Klene, J.E. Knox, J.B. Cross, V. Bakken, C. Adamo, J. Jaramillo, R. Gomperts, R.E. Stratmann, O. Yazyev, A.J. Austin, R. Cammi, C. Pomelli, J.W. Ochterski, R.L. Martin, K. Morokuma, V.G. Zakrzewski, G.A. Voth, P. Salvador, J.J. Dannenberg, S. Dapprich, A.D. Daniels, Ö. Farkas, J.B. Foresman, J.V. Ortiz, J. Cioslowski, D.J. Fox, *Gaussian 09*, Revision D.01, Gaussian, Inc., Wallingford, CT, 2009.
- [¹⁷] F. Weigend, R. Ahlrichs, Balanced basis sets of split valence, triple zeta valence and quadruple zeta valence quality for H to Rn: Design and assessment of accuracy, *Phys. Chem. Chem. Phys.* 7 (2005) 3297-3305, <https://doi.org/10.1039/B508541A>

- [¹⁸] A.V. Marenich, C.J. Cramer, D.G. Truhlar, Universal solvation model based on solute electron density and on a continuum model of the solvent defined by the bulk dielectric constant and atomic surface tensions, *J. Phys. Chem. B* 113 (2009) 6378-6396, <https://doi.org/10.1021/jp810292n>
- [¹⁹] R.E. Skyner, J.L. McDonagh, C.R. Groom, T. van Mourik, J.B.O. Mitchell, A review of methods for the calculation of solution free energies and the modelling of systems in solution. *Phys. Chem. Chem. Phys.* 17 (2015) 6174-6191, <https://doi.org/10.1039/C5CP00288E>
- [²⁰] W.J. Hehre, *A Guide to Molecular Mechanisms and Quantum Chemical Calculations*, Wavefunction Inc., Irvine, CA, USA, 2003, p. 153, 181.
- [²¹] A. Endo, M. Kajitani, M. Mukaida, K. Shimizu, G.P. Sato, A New Synthetic Method for Ruthenium Complexes of β -Diketones from 'Ruthenium Blue Solution' and their Properties, *Inorg. Chim. Acta*, 150 (1988) 25-34, [https://doi.org/10.1016/S0020-1693\(00\)87620-3](https://doi.org/10.1016/S0020-1693(00)87620-3)
- [²²] D. Das, A.K. Das, B. Sarkar, T.K. Mondal, S.M. Mobin, J. Fiedler, S. Zalis, F.A. Urbanos, R. Jimenez-Aparicio, W. Kaim, G.K. Lahiri, The Semiquinone-Ruthenium Combination as a Remarkably Invariant Feature in the Redox and Substitution Series $[\text{Ru}(\text{Q})_n(\text{acac})_{3-n}]^m$, $n = 1-3$; $m = (-2), -1, 0, +1, (+2)$; $\text{Q} = 4,6\text{-Di-}i\text{-tert-butyl-}N\text{-phenyl-}o\text{-iminobenzoquinone}$, *Inorg. Chem.* 48 (2009) 11853-11864, <https://doi.org/10.1021/ic901900g>
- [²³] R.R. Gagné, C.A. Koval, G.C. Lisensky, Transferability of ligand field parameters and nonlinear ligation in chromium(III) complexes, *Inorg. Chem.* 19 (1980) 2855-2857, <http://dx.doi.org/10.1021/ic50211a081>
- [²⁴] M. Landman, R. Liu, R. Fraser, P.H. van Rooyen, J. Conradie, *Fac* and *Mer* Fischer DPPE-Carbene complexes of chromium: X-ray, DFT and electrochemical study, *J. Organomet. Chem.* 752 (2014) 171-182, <https://doi.org/10.1016/j.jorganchem.2013.12.003>
- [²⁵] K.C. Kemp, E. Fourie, J. Conradie, J.C. Swarts, Ruthenocene-containing beta-diketones: synthesis, pK_a' values, keto-enol isomerisation kinetics and electrochemical aspects, *Organometallics* 27 (2008) 353-362, <http://dx.doi.org/10.1021/om700609z>
- [²⁶] E. Eskelinen, P. Da Costa, M. Haukka, The synthesis and electrochemical behavior of ruthenium(III) bipyridine complexes: $[\text{Ru}(\text{dcbpy})\text{Cl}_4]^-$ (dcbpy = 4,4'-dicarboxylic acid-2,2'-bipyridine) and $[\text{Ru}(\text{bpy})\text{Cl}_3\text{L}]$ ($\text{L} = \text{CH}_3\text{OH}, \text{PPh}_3, 4,4'\text{-bpy}, \text{CH}_3\text{CN}$), *J. Electroanal. Chem.* 579 (2005) 257-265, <http://dx.doi.org/10.1016/j.jelechem.2005.02.014>
- [²⁷] B.M. Holligan, J.C. Jeffery, M.K. Norgett, E. Schatz, M.D. Ward, The Co-ordination Chemistry of Mixed Pyridine-Phenol Ligands: Spectroscopic and Redox Properties of Mononuclear Ruthenium Complexes with $(\text{Pyridine})_{6-x}, (\text{Phenolate})_x$, Donor Sets ($x = 1$ or 2), *J. Chem. Soc. Dalton Trans.* (1992) 3345-3351, <http://dx.doi.org/10.1039/DT9920003345>;

- D.P. Rillema, D.S. Jones, H.A. Levy, Structure of Tris(2,2'-bipyridyl)ruthenium(II) Hexafluorophosphate, $[\text{Ru}(\text{bipy})_3] [\text{PF}_6]_2$, X-Ray Crystallographic Determination, J. Chem. Soc., Chem. Commun. (1979) 849-850, <https://doi.org/10.1039C39790000849>;
- G.K. Lahiri, S. Bhattacharya, B.K. Ghosh, A. Chakravorty, Ruthenium and Osmium Complexes of N,O Chelators: Syntheses, Oxidation Levels, and Distortion Parameters, Inorg. Chem. 26 (1987) 4324-4331, <https://doi.org/10.1021ic00273a010>;
- N. Bag, G.K. Lahiri, S. Bhattacharya, L.R. Falvello, A. Chakravorty, Ruthenium Phenolates. Chemistry of a Family of $\text{Ru}^{\text{III}}\text{O}_6$ Tris Chelates, Inorg. Chem. 27 (1988) 4396-3365, <https://doi.org/10.1021ic00267a028>;
- P. Ghosh, A. Pramanik, N. Bag, G.K. Lahiri, A. Chakravorty, Bidentate ligand substitution in $\text{PhCCo}_3(\text{CO})_9$. Synthesis, molecular structure, and redox reactivity of $\text{PhCCo}_3(\text{CO})_7(\text{cis-Ph}_2\text{PCH=CHPh}_2)$, J. Organomet. Chem. 454 (1993) 273-280, [https://doi.org/10.10160022-328X\(93\)83251-P](https://doi.org/10.10160022-328X(93)83251-P);
- G.K. Lahiri, S. Bhattacharya, M. Mukherjee, A.K. Mukherjee, A. Chakravorty, Directed Metal Oxidation Levels in Azo-Ruthenium Cyclometalates. Synthesis and Structure of a Trivalent Family, Inorg. Chem. 26 (1987) 3359-3365, <https://doi.org/10.1021ic00267a028>;
- S. Chattopadhyay, N. Bag, P. Basu, G.K. Lahiri, A. Chakravorty, Oxo Transfer and Metal Oxidation in the Reaction of $[\text{Ru}(\text{PPh}_3)_3\text{Cl}_2]$ with *m*-Chloroperbenzoic Acid: Structure of $[\text{Ru}(\text{PPh}_3)_2(\text{m-CIC}_6\text{H}_4\text{CO}_2)\text{Cl}_2]$, J. Chem. Soc., Dalton Trans. (1990) 3389-3392, <https://doi.org/10.103-DT9900003389>